Journal of Luminescence 166 (2015) 117–122

Contents lists available at ScienceDirect

Journal of Luminescence

journal homepage: www.elsevier.com/locate/jlumin

# Energy migration processes in undoped and Ce-doped multi-component garnet single crystal scintillators

K. Bartosiewicz [a,b,*], V. Babin [a], K. Kamada [c], A. Yoshikawa [c,d], M. Nikl [a]

[a] Institute of Physics AS CR, Cukrovarnicka 10, Prague 16253, Czech Republic
[b] Faculty of Nuclear Sciences and Physical Engineering, Czech Technical University in Prague, Brehova 7, Praha 1 11519, Czech Republic
[c] NICHe, Tohoku University, 6-6-10 Aoba, Aramaki, Aoba-ku, Sendai 980-8579, Japan
[d] Institute for Materials Research (IMR), Tohoku University, Sendai 980-8577, Japan

ARTICLE INFO

*Article history:*
Received 17 October 2014
Received in revised form
5 May 2015
Accepted 10 May 2015
Available online 18 May 2015

*Keywords:*
Multicomponent garnets
$Ce^{3+}$
Luminescence
Energy transfer

ABSTRACT

Multicomponent garnets ($Y_{3-x}Gd_xAl_{5-y}Ga_yO_{12}$) doped with $Ce^{3+}$ ions are promising scintillators with a high density, fast response time and high light yield. To deepen the knowledge about the transfer stage of scintillation mechanism we discuss the energy migration and energy transfer processes in the set of undoped and $Ce^{3+}$ activated multicomponent garnet single crystals. Temperature dependence of $Gd^{3+}$ emission intensities as well as decay kinetics in $Y_{3-x}Gd_xAl_{5-y}Ga_yO_{12}$ ($x,y=1,2,3$) crystals point to the $Gd^{3+} \rightarrow Gd^{3+}$ nonradiative energy migration, which is diffusion limited. Concentration quenching of $Gd^{3+}$ emission occurs by energy migration to accidental impurities and/or structure defects. Temperature dependence of photoluminescence emission intensities and decay time measurements of $Gd^{3+}$ as well as $Ce^{3+}$ ions in $Gd_3Ga_3Al_2O_{12}:Ce^{3+}$ single crystal reveal nonradiative energy transfer $Gd^{3+} \rightarrow Ce^{3+}$ (including migration through $Gd^{3+}$ sublattice) which is responsible for slow $Ce^{3+}$ fluorescence decay component.



## 1. Introduction

Research and development of new scintillator materials is mainly triggered by the growing needs of modern medical imagining, homeland security and high energy physics. During the last two decades, new types of scintillators, in particular, Ce-doped inorganic scintillators were intensively studied and some of them were successfully developed for commercial production, for recent reviews see Refs. [1,2]. An important class of scintillators are the aluminum garnets doped with lanthanide ions. The garnets have good chemical and radiation stability, excellent mechanical properties and show efficient luminescence when doped with lanthanide ions. Autrata et al. [3] and Moszynski et al. [4] showed potential of $Ce^{3+}$-doped $Y_3Al_5O_{12}$ (YAG) single crystal for fast scintillators. Research of the $Ce^{3+}$-and $Pr^{3+}$-doped YAG host revealed the absence of nonradiative thermal quenching up to 550 K and 250 K, respectively [5]. However, YAG has relatively low density ($\rho=4.56$ g/cm$^3$) and effective atomic number ($Z_{eff}=32.6$). Isostructural $Lu_3Al_5O_{12}$ (LuAG) has a higher density ($\rho=6.67$ g/cm$^3$) and effective atomic number ($Z_{eff}=63$), which is advantageous in the case of high energy gamma-ray detection [6]. However, experimental studies reported light yield (LY) value for $Ce^{3+}$ activated YAG and LuAG of about 25,000 phot/MeV and 12,500 phot/MeV, respectively [7], which is far below their theoretical value of about 60,000 phot/MeV calculated by Bartram–Lempicki equation [8]. The discrepancy is due to delayed recombination process caused by electron trapping at various electron traps related e.g. to the $Y_{Al}$ and $Lu_{Al}$ antisite defects (Y and Lu cations localized in octahedral sites of the Al cations) in the host lattice. Their presence was proved by both experiments and theoretical calculations [9–11]. The higher melting temperature and smaller difference between $Lu^{3+}$ and $Al^{3+}$ radii might result in a higher concentration of antisite defect-related traps in LuAG host with respect to YAG: taking also into account their increased thermal depth, such defects might have a greater detrimental effect on the energy transfer to $Ce^{3+}$ ions. This could explain the lower light yield of LuAG:Ce with respect to that of YAG:Ce and enhanced presence of slow components in scintillation decay in the former compound [12,13]. The latest studies of $Ce^{3+}$-doped scintillators based on heavy aluminum garnets (LuAG:Ce) revealed that $Ce^{3+}$ concentration as well as optimization of manufacturer technology has an influence on the light yield value. An essential improvement was demonstrated in samples containing $>0.2$ at% of Ce; the light yield measured in LuAG:Ce (0.55 at%) was about 26,000 phot/MeV, for samples obtained from both Bridgman and Czochralski methods [14]. $Pr^{3+}$-doped LuAG single crystals were introduced in 2005 [15] and 2006 [16], prepared by micro-pulling-down and Czochralski

* Corresponding author at: Institute of Physics AS CR, Cukrovarnicka 10, Prague 16253, Czech Republic. Tel.: +420 220 318 440.
*E-mail address:* bartosiewicz@fzu.cz (K. Bartosiewicz).

http://dx.doi.org/10.1016/j.jlumin.2015.05.015
0022-2313/

techniques, respectively. Several groups [17–24] studied scintillation characteristic of LuAG:Pr and found them very promising due to favorable combination of fast scintillation decay dominated by 20 ns component and light yield approaching 20,000 phot/MeV with energy resolution 4.6%@662 keV. Moreover, its scintillation parameters do not deteriorate significantly up to 300 °C [25]. In recent years, by the "band-gap engineering" and tuning the $Ce^{3+}$ energy level position strategy [26,27], dramatic improvement of the scintillation performances has been achieved compared to simple aluminum garnet scintillators. For example, $Ga^{3+}$ admixture can suppress the effects of shallow electron traps (such as antisite defects) which get buried in the conduction band, as the bottom of the conduction band gets lower in energy while the $5d_1$ level of $Ce^{3+}$ gets higher. In contrast, the Gd admixture lowers the position of the $5d_1$ level of $Ce^{3+}$ and secures sufficient separation of $5d_1$ level from the bottom of the host conduction band even for Ga-rich composition to prevent the excited state ionization of $Ce^{3+}$ emission center around room temperature (RT). Consequently, the derived $(Gd,Lu)_3(Ga,Al)_5O_{12}$:Ce material system gave rise to high figure-of-merit scintillators. Udea et al. [28] and Ogieglo et al. [29] studied the influence of replacing $Al^{3+}$ by $Ga^{3+}$ in multicomponent garnets doped with $Ce^{3+}$. They demonstrated the dependence of the energy levels of the 5d state position relative to the conduction band in these materials on the Ga content. With increasing Ga content in the Ce-doped multicomponent garnets, the $5d_1$ level and the conduction band become close because of the decrease in the crystal field strength and band gap, resulting in luminescence quenching by the thermal ionization. In 2012 Czochralski-grown 2-inch diameter $Gd_3Ga_3Al_2O_{12}$:Ce (GGAG:Ce) single crystal was obtained [21], which showed excellent characteristics, including high density 6.63 g/cm$^3$, high light yield around 46,000 phot/MeV (this value is by 30–40% more than the value of the best LYSO:Ce scintillator reported so far), and excellent energy resolution 4.9%@622 keV. The advantage of these scintillators is their very fast and intensive $5d\rightarrow4f$ emission transitions of $Ce^{3+}$ centers in the green–yellow spectral range with dominating decay time about 50–60 ns. However, slow micro-millisecond emission of $Gd^{3+}$ ions was observed at 310 nm due to forbidden $4f\rightarrow4f$ transition of $Gd^{3+}$. At low concentration both $Ce^{3+}$ and $Gd^{3+}$ take part in the emission processes in the visible and ultraviolet spectral ranges, respectively. In slightly Ce–Gd co-doped YAG or LuAG they mutually compete for the excitation energy capture. At high concentration of $Gd^{3+}$ ions in undoped material, their emission is suppressed by energy migration and concentration quenching in the Gd-sublattice. The energy transfer towards $Ce^{3+}$ centers has also been observed at room temperature [30,31]. The $Gd^{3+}$ ions are well-known as effective donors for a number of rare earth ions [32]. Hence, the energy transfer from $Gd^{3+}$ to $Ce^{3+}$ ions can also be expected in Gd–Ce co-doped multicomponent garnets, further mediated by the energy migration in the Gd-sublattice [30,31]. On the other hand, in the case of the $Pr^{3+}$-doped $Gd^{3+}$ containing multicomponent garnets, much worse scintillation performance was reported, namely the light yield values decrease down to 4000–4500 phot/MeV [21,33], due to resonance of the $5d_1\rightarrow{}^3H_4$ emission transition of $Pr^{3+}$ and $^8S\rightarrow{}^6P_x$ absorption transitions of $Gd^{3+}$ within 302–314 nm, which creates an additional nonradiative pathways away from the $5d_1$ state of $Pr^{3+}$ [34,35].

The aim of this paper is to measure temperature dependence of $Gd^{3+}$ emission intensities and decay times related to its $^6P_x\rightarrow{}^8S$ 4f–4f transition peaking at 313 nm at the set of undoped matrices with variable content of Gd and Ga cations. At room temperature both the emission intensity and decay time of 313 nm emission line are greatly dependent on the Gd content in an undoped multicomponent garnet host [34]. Furthermore, for a selected identical host composition the Ce-doped sample is measured as well. Energy migration over the $Gd^{3+}$ sublattice and its transfer towards $Ce^{3+}$ centers is thus studied in a great detail.

## 2. Experimental

All the undoped and $Ce^{3+}$-doped $Y_{3-x}Gd_xAl_{5-y}Ga_yO_{12}$ ($x$, $y=1,2,3$) were prepared by micro-pulling-down method [26,27] in Japanese laboratory. Polished plates of approx. ⌀ 2.7 mm × 0.7 mm cut from the parent rods were used for all the measurements.

Absorption spectra were measured by the Shimadzu 3101PC spectrometer in the 200–800 nm range. The photoluminescence (PL) spectra were measured in the temperature range 8–300 K, PL decay kinetics were measured in the range 8–500 K using the custom made 5000M Horiba Jobin Yvon fluorescence spectrometer. Janis closed cycle cryostat was used in all the experiments. In the steady state spectra measurements, the sample was excited by deuterium lamp (Heraus Gmbh). All PL spectra were corrected for the spectral distortions of the setup. In slow decay kinetics measurements the microsecond xenon flashlamp was used and signal was recorded by means of multichannel scaling method. True decay times were obtained using the convolution of the instrumental response function with an exponential function and the least-square-sum-based fitting program (SpectraSolve software package).

## 3. Results and discussion

### 3.1. Undoped $Y_{3-x}Gd_xAl_{5-y}Ga_yO_{12}$ ($x,y=1,2,3$) samples

In Fig. 1 typical room temperature absorption spectrum of $Gd_2Y_1Ga_1Al_4O_{12}$ single crystal is given. There are three narrow absorption lines around 246, 275 and 310 nm, which are attribute to the transition from $^8S_{7/2}\rightarrow{}^6D_J$, $^8S_{7/2}\rightarrow{}^6I_J$, and $^8S_{7/2}\rightarrow{}^6P_J$ of $Gd^{3+}$, respectively. Besides, a strong absorption of host lattice (HL) is observed below 220 nm.

In Fig. 2 the normalized excitation and emission spectra of $Gd_2Y_1Ga_1Al_4O_{12}$ single crystal are given at 8 K. The excitation spectrum was monitored at the maximum of $Gd^{3+}$ emission at 313 nm. It consists of sharp peaks related to $^8S_{7/2}\rightarrow{}^6D_J$ and $^8S_{7/2}\rightarrow{}^6I_J$ transitions around 240 nm and 270 nm, respectively. The photoluminescence (PL) emission spectrum was excited in $Gd^{3+}$ (4f–4f) absorption at 275 nm. Upon excitation in the $^6I_J$ level at 8 K, emission from the lowest energy $^6P_{7/2}$ component with maximum around 313 was observed. The critical distance, $R_c$, for $Gd^{3+}\rightarrow Gd^{3+}$ energy transfer was derived by studying the influence of a dilution of the $Gd^{3+}$ sublattice by optically inactive $Y^{3+}$ ions on the luminescence properties. This approach is discussed in detail in Ref. [36] and shows that for oxides $R_c$ is around 6.5 Å. Efficient

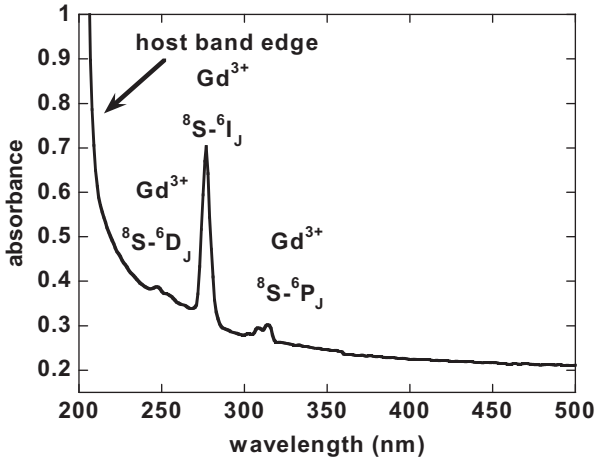


**Fig. 1.** Absorption spectrum of $Gd_2Y_1Ga_1Al_4O_{12}$ single crystal.

energy migration is only to be expected in gadolinium compounds where the $Gd^{3+}$–$Gd^{3+}$ distance is less than the value of $R_c$ mentioned above. Fig. 3 shows integrals of PL spectra and evaluated decay times as a function of temperature. For $Gd_1Y_2Gd_1Al_4O_{12}$ all decay curves were single-exponential. In several cases e.g. $Gd_2Y_1Gd_1Al_4O_{12}$, the decay curves possessed non-exponential character and could be only fit by several exponential components. In such cases, mean decay time $\tau_m$ was introduced for consideration, defined by the equation

$$\tau_m = \frac{\sum A_i \tau_i^2}{\sum A_i \tau_i} \quad (1)$$

where $A$ is the amplitude and $\tau$ is the decay time value from the fit. With increasing temperature both emission intensities and decay times are decreasing, but their behavior is different for different Gd content. For $Gd_1Y_2Gd_1Al_4O_{12}$ only mild decrease in PL intensities and decay times is observed, while for $Gd_2Y_1Gd_1Al_4O_{12}$ sharp decline is observed within 30–60 K. In all undoped samples the same relationship was observed, namely the intensities and decay times of $Gd^{3+}$ emission decreases with increasing $Gd^{3+}$ concentration as well as temperature. The results are in good agreement with other studies, which have shown that in $Gd^{3+}$ garnets at least 50% of the $Y^{3+}$ sites should be occupied by $Gd^{3+}$ ions to allow for efficient energy migration among the $Gd^{3+}$ ions [34,36].

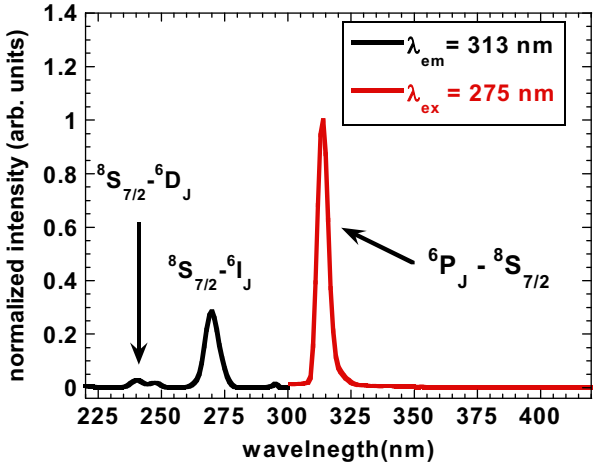


**Fig. 2.** Excitation and emission spectra (measured at maxima of emission or excitation peaks at $\lambda_{em}$=313 nm and $\lambda_{ex}$=275 nm, respectively) of $Gd_2Y_1Ga_1Al_4O_{12}$ single crystal.

Such dependence clearly points to concentration quenching in the $Gd^{3+}$ sublattice. At high enough concentration of $Gd^{3+}$ ions, there is a sufficient reduction of the average distance between these luminescence centers to favor energy migration in the Gd sublattice. Due to very efficient and fast $Gd^{3+} \rightarrow Gd^{3+}$ energy transfer, the excitation energy can migrate along a large number of centers before being emitted. However, there is a certain concentration of defects/traps that can act as acceptors, so that the excitation energy from Gd-sublattice can finally be transferred to them. These centers can relax to their ground state nonradiatively or eventually by an infrared emission. Thus, they act as an energy sink within the transfer chain and the $Gd^{3+}$ luminescence becomes quenched. These kinds of acceptor centers are called killers or quenching traps. In order to explore this presumed energy migration, we take the temperature dependence of PL intensities into account. As can be seen from Fig. 4 at low temperature energy migration is very weak, but at 100 K it is efficient. The temperature dependence can be explained in this way: due to inhomogeneous broadening caused by local fluctuation of crystal field strength and site symmetry (due to atomistic fluctuation of Gd–Y and Ga–Al site occupancies), the $^6P_{7/2} \rightarrow {}^8S_{7/2}$ transitions of $Gd^{3+}$ ions are not exactly in resonance, but their transition energies show very small mismatches. Phonons are required to overcome them. At room temperature, the absorption and emission lines of $Gd^{3+}$ ions are broadened due to available phonons, their overlap becomes large enough to enable the energy transfer between the $Gd^{3+}$ neighboring ions and energy migration process can occur.

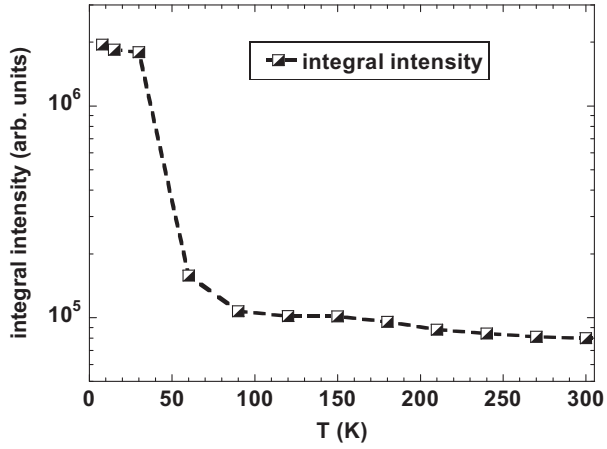


**Fig. 4.** The temperature dependence of PL integral intensities of $Gd^{3+}$ emission in the $Gd_2Y_1Ga_3Al_2O_{12}$ single crystal under excitation at 275 nm.

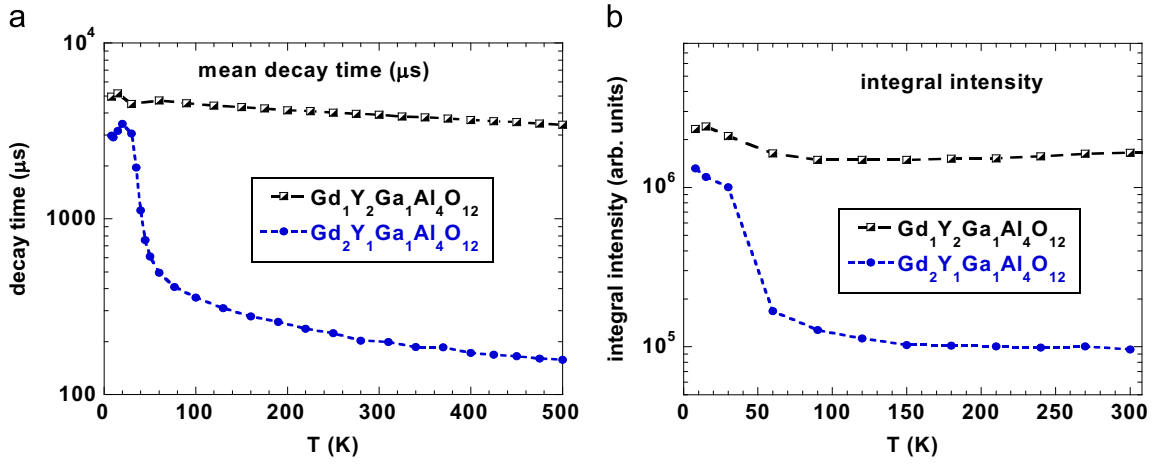


**Fig. 3.** The temperature dependence of $Gd^{3+}$ decay times (a) and PL integral intensities (b) in the $Gd_1Y_2Ga_1Al_4O_{12}$ and $Gd_2Y_1Ga_1Al_4O_{12}$ single crystals; the samples were excited at $\lambda_{ex}$=275 nm and monitored at $\lambda_{em}$=313 nm.

However, at very low temperatures, due to lack of active phonon modes and low overlap, the energy migration is hampered [32]. Consequently, the efficient ET processes require the assistance of lattice phonons and electron–phonon coupling needs to be considered. Such phonon-assisted ET process is temperature dependent and its efficiency rises up to higher temperatures [32,37]. The decay time of the $Gd^{3+}$ emission at 313 nm in $Gd_2Y_1Ga_1Al_4O_{12}$ single crystal slightly increases from 8 K to 30 K; this can be connected with the thermal population of higher energy levels from where the transitions are less allowed [38,39]. Figs. 3b and 4 show the integrals of PL emission intensity of $Gd^{3+}$ ion under excitation at 275 nm in $Gd_2Y_1Ga_1Al_4O_{12}$ and $Gd_2Y_1Ga_3Al_2O_{12}$ crystals. It is observed that the behavior of both curves in the entire temperature range (8–300 K) is almost identical. Namely, in both samples the sharp and mild declines of $Gd^{3+}$ emission intensities are observed within 30–60 K and 60–300 K, respectively. This observation reveals that the replacing of $Al^{3+}$ by $Ga^{3+}$ has a rather negligible influence on the $Gd^{3+}$ features in $Y_{3-x}Gd_xAl_{5-y}Ga_yO_{12}$ hosts. Fig. 5 shows the decay curves of the $Gd^{3+}$ ions in $Gd_2Y_1Ga_1Al_4O_{12}$ crystal at different temperatures. It can be seen from this figure that with increasing temperature the decay curve of 313 nm emission line of $Gd^{3+}$ ions accelerates. At 35 K the mean decay time of $Gd^{3+}$ emission obtained from multi-exponential approximation shows only about half of its low temperature limit i.e. the value of decay time of $Gd^{3+}$ emission observed at 8 K. The decay curves of $Gd_2Y_1Ga_1Al_4O_{12}$ were fit to the following double exponential function:

$$I = I_0\exp(-t/\tau) + I_0'\exp(-t/\tau') \quad (2)$$

where $I$ is the luminescence intensity, $I_0$, $I_0'$ are the intensities at 0 μs, $t$ is the time and $\tau,\tau'$ are decay times. Furthermore, the decay curve of $Gd^{3+}$ emission recorded at 8 K shows an initial rise. Given the fact that excitation is into $^6I_J$ multiplet at 275 nm, but emission is due to radiative transition from lower lying multiplet sublevel $^6P_{7/2}$ the observed rising part in the decay is most probably due to intracenter transition $^6I_J \rightarrow {}^6P_{5/2}$. Energy barrier for such a transition is apparently very small as it is no more visible at 35 K. The results show that at low temperature the decay occurs generally by radiative transitions in the excited centers. Energy transfer is hampered. At higher temperatures the decay is much faster than expected for radiative decay of isolated ions [40]. Energy migration among the $Gd^{3+}$ sublattice occurs and brings the excitation energy to killer sites. An analysis of curves presented on Figs. 4 and 5 shows that: (i) at lowest temperatures energy migration among the $Gd^{3+}$ ions is hampered and the decay occurs generally by radiative transitions in the excited $Gd^{3+}$ centers (ii) decay curves show multiexponential character in the entire temperature range, and (iii) assistance of phonons is needed to enable efficient energy migration among $Gd^{3+}$ ions. We are dealing with the diffusion-limited energy migration [41–43].

### 3.2. Undoped and Ce-doped $Gd_3Ga_3Al_2O_{12}$ samples

In Fig. 6 the normalized excitation and emission spectra of $Gd_3Ga_3Al_2O_{12}:Ce^{3+}$ single crystal are given at 8 K. The excitation spectrum was monitored at a maximum of $Gd^{3+}$ emission at 315 nm. It consists of sharp peaks related to $^8S_{7/2} \rightarrow {}^6D_J$ and $^8S_{7/2} \rightarrow {}^6I_J$ transitions around 240 nm and 270 nm, respectively. The PL spectrum of $Gd_3Ga_3Al_2O_{12}:Ce^{3+}$ was excited at $Gd^{3+}$ (4f–4f) absorption line at 270 nm. The observed band with maximum at around 525 nm is typical for $5d_1 \rightarrow {}^2F_{5/2}$, $^2F_{7/2}$ emission of $Ce^{3+}$ ions in garnets. The intense and narrow peak with maximum around 315 nm is typical for $^6P_J \rightarrow {}^8S_{7/2}$ emission of $Gd^{3+}$. Broad emission band peaking around 390 nm is also observed. Though the origin of this host-related emission is not clear, it might be easily related to the excitons localized around impurities [44] or structural defects [45]. The PL emission spectrum excited at 270 nm besides typical $4f \rightarrow 4f$ $Gd^{3+}$ emission, exhibits also typical $Ce^{3+}$ emission. This evokes an idea of possible ET from $Gd^{3+}$ to $Ce^{3+}$. In order to explore this presumed energy transfer from $Gd^{3+}$ to $Ce^{3+}$, the PLE spectrum monitored at a maximum of $Ce^{3+}$ emission at 520 nm was performed. The PLE spectra of the $Ce^{3+}$ emission from $Gd_3Ga_3Al_2O_{12}$:Ce sample are shown in Fig. 7. Two dominant bands observed in these spectra are related to the well-known $4f \rightarrow 5d_1$ (between 390 and 480 nm) and $4f \rightarrow 5d_2$ (between 315 and 360 nm) transitions of $Ce^{3+}$, respectively. Weak line at 270 nm is due to $^8S_{7/2} \rightarrow {}^6P_J$ transition of $Gd^{3+}$ ions. Its presence in the excitation spectra indicate that the energy transfer from the $Gd^{3+}$ to $Ce^{3+}$ ions takes place in the $Gd_3Ga_3Al_2O_{12}:Ce^{3+}$ single crystal similarly what was observed in Ref. [30]. From these spectra we observe that the intensity ratio of $(4f \rightarrow 5d_2)/(4f \rightarrow 5d_1)$ is two times less at RT than that at 8 K. A similar changes of intensity ratio of Ce-related bands as a function of temperature was reported before for $Y_3Al_5O_{12}:Ce^{3+}$ and this thermal behavior was explained in terms that $Ce^{3+}$ occupies a tetragonally distorted cubic site in this host. Due to this distortion, the $^2F_{5/2}$ ground sate of $Ce^{3+}$ is additionally split into E′ and E″ levels [46]. At low temperature, only the lowest ground state E″(4f) will be populated. Since the dipole moment for the transition $4f(E') \rightarrow 5d_2$ is much smaller than that for $4f(E'') \rightarrow 5d_1$ the oscillator strength of the absorption band near 340 nm is predicted to be low at low temperature. As temperature increases and the state E′(4f) becomes thermally populated the oscillator strength for the 340 nm band should increase rapidly because the transitions $4f(E') \rightarrow 5d_2$ is strongly allowed while the

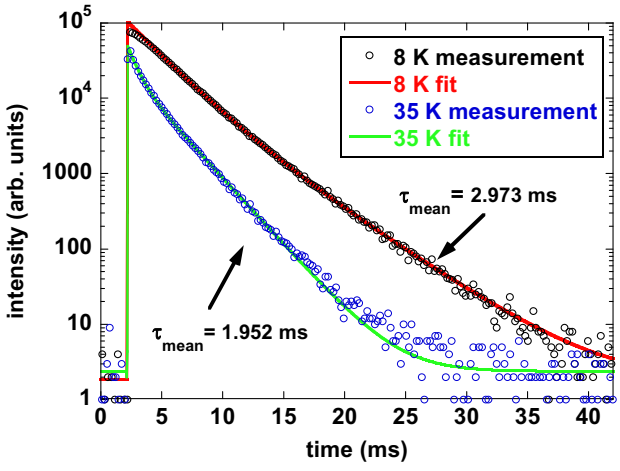


**Fig. 5.** Decay curves of the intrinsic $Gd^{3+}$ emission in $Gd_2Y_1Ga_1Al_4O_{12}$ single crystal as a function of temperature; the sample was excited at $\lambda_{ex}$=275 nm and monitored at $\lambda_{em}$=313 nm. Solid lines are two-exponential approximations.

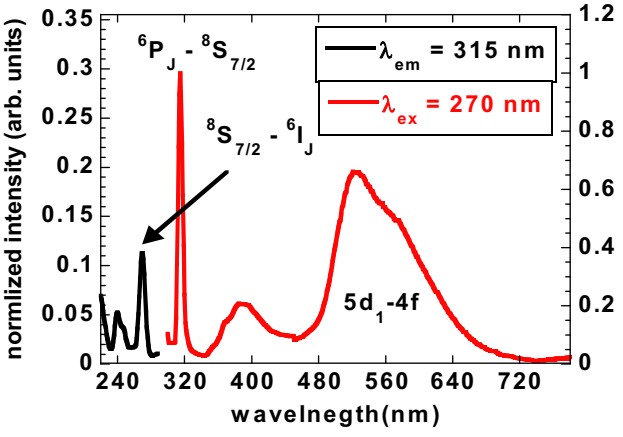


**Fig. 6.** Excitation and emission spectra (measured at maxima of emission or excitation peaks at 315 nm and 270 nm, respectively) of $Gd_3Ga_3Al_2O_{12}:Ce^{3+}$ single crystal.

opposite holds for 4f(E′)→5d$_1$ [46]. Furthermore, the intensity of Gd-related line around 270 nm is 3.5 times higher at RT than that at 8 K. The increase of PLE intensity in $^8S_{7/2}\rightarrow{}^6P_J$ absorption transition indicates that the efficiency of ET $Gd^{3+}\rightarrow Ce^{3+}$ rises with increasing temperature. This assumption is confirmed further by investigations of temperature dependence of emission intensities as well as decay times. The temperature dependence of PL decays of $Gd^{3+}$ emission line at 315 nm was performed for the undoped as well as for Ce-doped $Gd_3Ga_3Al_2O_{12}$ samples, see Fig. 8. For the Ce-doped sample, the decay time shortened much faster, becoming at 60 K as much as 190 times shorter than that in the undoped sample. The PL decay time for $Gd^{3+}$ at 315 nm as well as for $Ce^{3+}$ at 520 nm was measured under excitation at $^8S_{7/2}\rightarrow{}^6I_J$ ($Gd^{3+}$) absorption line at 270 nm, representing very similar behavior and values, except the range 8–30 K, where $Ce^{3+}$-related decay times are somewhat shorter, see Fig. 9. In Gd-concentrated samples ET is carried out by two different ways which act together: (i) first excitation energy migrate over Gd sublattice and is brought close to $Ce^{3+}$ ions, then (ii) due to spectral overlap of the $Gd^{3+}$ emission line with $Ce^{3+}$ 4f→5d$_2$ absorption band, the absorbed excitation energy is nonradiatively transferred to $Ce^{3+}$ ions.

In Fig. 9 we observe these mechanisms, because the decay times of $Ce^{3+}$ ion emission are the same as those of $Gd^{3+}$ ions i.e. of the order of millisecond ($Ce^{3+}$ ions copy exactly the behavior of $Gd^{3+}$ ions). At low temperatures their spectral overlap is minor and as a consequence the ET is less efficient (see temperature range 8–30 K), but at higher temperatures due to broadening of emission line and absorption band of $Gd^{3+}$ and $Ce^{3+}$ ions, respectively, the spectral overlap is sufficient to enable effective energy transfer. The temperature dependence of Gd-related emission line in undoped and Ce-doped $Gd_3Ga_3Al_2O_{12}$ shows very similar behavior in the range 8–60 K (Figs. 10 and 11). In both cases, in the range 8–30 K an increase of Gd-related emission line in $Gd_3Ga_3Al_2O_{12}$ and $Gd_3Ga_3Al_2O_{12}$:$Ce^{3+}$ could be observed. At higher temperatures, fast decrease of intensities was observed due to concentration quenching. In Ce-doped sample (Fig. 11), an emission intensities redistribution of Gd- and Ce-related line and band, respectively, is evident in the range 25–70 K, namely the intensity of Gd line is decreasing and at the same time the intensity of Ce band is increasing. Above 70 K, the $Gd^{3+}$ line is practically quenched and $Ce^{3+}$ band reaches its maximum intensity at about 120 K and slightly decreases around 300 K due to thermal quenching and/or thermal ionization. These characteristics evidence the energy transfer from $Gd^{3+}$ to $Ce^{3+}$ ions. According to the Forster–Dexter model of the interaction mechanism [32] the efficiency of $Gd^{3+}$ to $Ce^{3+}$ transfer is expected to be rather low because of minor spectral overlap between the $^6P_J\rightarrow{}^8S_{7/2}$ ($Gd^{3+}$) emission line and 4f→5d$_2$ ($Ce^{3+}$) absorption band.

However, Kucera et al. [30] and Blasse [47] have demonstrated that sharp $Gd^{3+}$ emission at 312 nm is located just at the edge of the broad $Ce^{3+}$ 4f→5d$_2$ absorption band. In such a case, it can be explained by: (i) with the temperature increase the corresponding absorption band of $Ce^{3+}$ and emission line of $Gd^{3+}$ become broader, and as a consequence their overlapping is larger and ET becomes more efficient [32]; (ii) the efficient ET process requires also assistance of lattice phonons and electron–phonon coupling

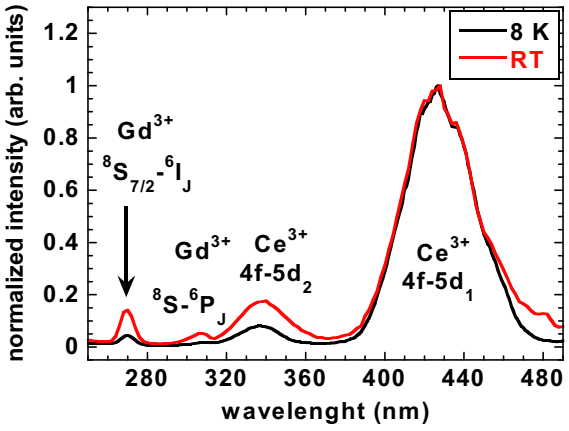


**Fig. 7.** Excitation spectra of $Gd_3Ga_3Al_2O_{12}$:$Ce^{3+}$ measured at 8 K and RT for the 520 nm emission of $Ce^{3+}$ ion.

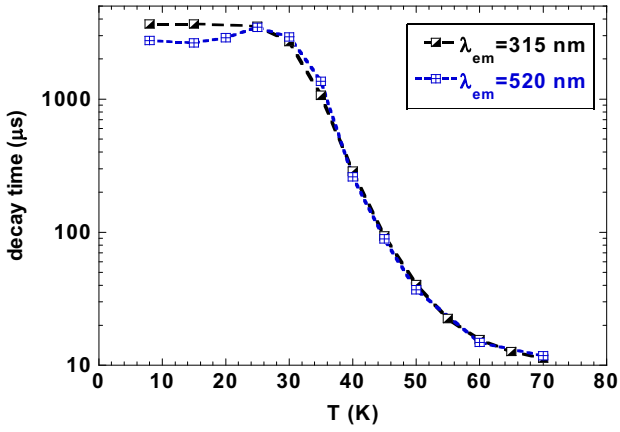


**Fig. 9.** The temperature dependence of PL decays of $Gd^{3+}$ ions; $\lambda_{ex}$=270 nm, $\lambda_{em}$=315 nm $^6P_J$($Gd^{3+}$) and $\lambda_{em}$=520 nm 5d$_1$($Ce^{3+}$) in $Gd_3Ga_3Al_2O_{12}$:$Ce^{3+}$ single crystal.

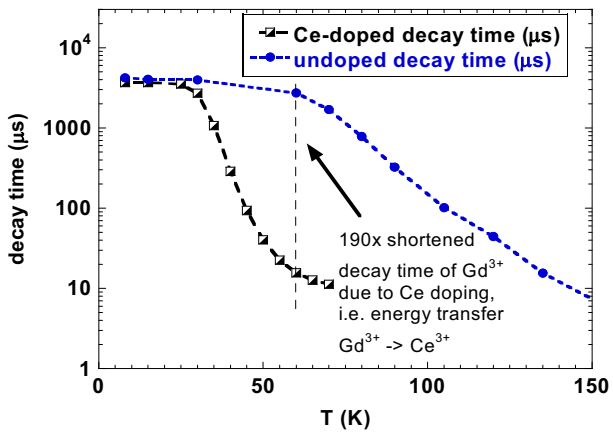


**Fig. 8.** The temperature dependence of PL decays of $Gd^{3+}$ ion ($\lambda_{ex}$=270 nm, $\lambda_{em}$=315 nm) in $Gd_3Ga_3Al_2O_{12}$:$Ce^{3+}$ and $Gd_3Ga_3Al_2O_{12}$ single crystals.

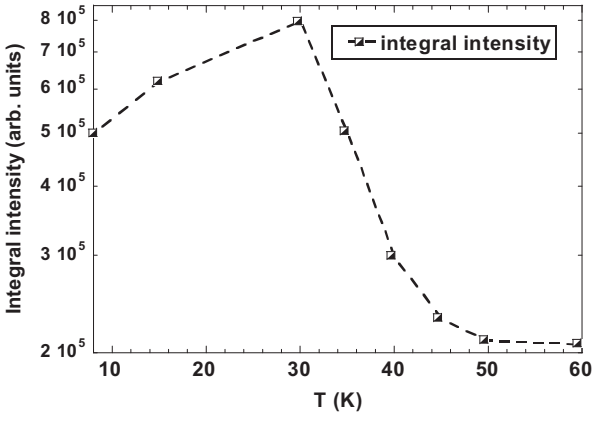


**Fig. 10.** The temperature dependence of PL integrals intensities of $Gd^{3+}$ emission related to 4f–4f transition under excitation at 270 nm in $Gd_3Ga_3Al_2O_{12}$ single crystal.

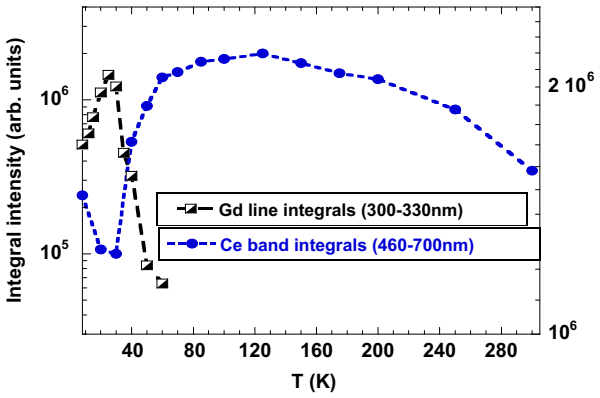


**Fig. 11.** The temperature dependence of PL emission intensities of Gd- and Ce-related line and band, respectively, under excitation at 270 nm in $Gd_3Ga_3Al_2O_{12}:Ce^{3+}$.

needs to be considered. Such phonons are available at higher temperature and enhance the observed ET [30].

## 4. Conclusions

The absorption and luminescence properties of undoped and Ce-doped multicomponent garnets ($Y_{3-x}Gd_xAl_{5-y}Ga_yO_{12}$) single crystals are investigated upon partial or total substitution of $Y^{3+}$ by $Gd^{3+}$ and $Al^{3+}$ by $Ga^{3+}$. Absorption, excitation and emission spectra as well as decay time measurements allow for detailed investigation of luminescent properties. Temperature dependence of photoluminescence emission intensity and decay time measurements in $Y_{3-x}Gd_xAl_{5-y}Ga_yO_{12}$ ($x,y=1,2,3$) point to the fact that the diffusion limited energy migration through the Gd sublattice takes place in samples in which two or three Y atoms are replaced by Gd ones in chemical formula. Its efficiency increases with the raising temperature due to an improvement of the resonant conditions among $^6P_J$ ($Gd^{3+}$) levels and assistance of available phonons at higher temperature. At low temperature $Gd^{3+}\rightarrow Gd^{3+}$ energy transfer is hampered due to small energy mismatches between neighboring $Gd^{3+}$ ions resulting from inhomogeneous broadening caused by local fluctuation of crystal field strength and site symmetry. At higher temperature the excitation energy diffuses among $Gd^{3+}$ ions, and gets trapped by unwanted impurities and/or structure defects and concentration quenching occurs. Furthermore, the replacing of $Al^{3+}$ by $Ga^{3+}$ has a rather negligible influence on the $Gd^{3+}$ emission features in $Y_{3-x}Gd_xAl_{5-y}Ga_yO_{12}$ ($x,y=1,2,3$) hosts. The nonradiative $Gd^{3+}\rightarrow Ce^{3+}$ energy transfer occurs in $Gd_3Ga_3Al_2O_{12}:Ce^{3+}$ due to spectral overlapping of $^6P_J\rightarrow{}^8S_{7/2}$ ($Gd^{3+}$) emission line with $4f\rightarrow 5d_2$ ($Ce^{3+}$) absorption band. Its efficiency also increases with rising temperature due to improved spectral overlap mentioned above. The energy transfer is proved by: (i) presence of $Gd^{3+}$ absorption line in $Ce^{3+}$ excitation spectrum, (ii) presence of $Ce^{3+}$ emission bands under the selective excitation into $Gd^{3+}$ ions, and (iii) the decay time of $Gd^{3+}$ emission is significantly shortened in the presence of $Ce^{3+}$ ions as well as the latter emission shows millisecond decay component when excited via $Gd^{3+}$ ions. The excitation energy migrates among $Gd^{3+}$ ions until is finally captured by $Ce^{3+}$ ions and afterwards released by its characteristic green–yellow light.

## Acknowledgment

Financial support of Czech science foundation No. P204/12/0805 and EC Marie Curie Initial Training Network LUMINET, No. 316906, projects are gratefully acknowledged.

## References

[1] K. Kramer, P. Dorenbos, H. Gudel, C. van Eijk, J. Mater. Chem. 16 (2006) 2773.
[2] M. Nikl, Meas. Sci. Technol. 17 (2006) R37.
[3] R. Autrata, P. Schauer, J. Kvapil, J. Kvapil, J. Phys. E: Sci. Instrum. 11 (1978) 707.
[4] M. Moszynski, T. Ludziewski, D. Wolski, W. Klamra, L. Norlin, Nucl. Instrum. Methods Phys. Res. A 345 (1994) 461.
[5] M.J. Weber, Solid State Commun. 12 (1973) 741.
[6] M. Nikl, E. Mihokova, J.A. Mares, A. Vedda, M. Martini, Phys. Status Solidi 181 (2000) R10.
[7] J. Mares, A. Beitlerova, M. Nikl, N. Solovieva, C. D'Ambrosio, K. Blazek, P. Maly, K. Nejezchleb, F. de Notaristefani, Radiat. Meas. 38 (2004) 353.
[8] P. Dorembos, IEEE Trans. Nucl. Sci. 57 (2010) 1162.
[9] V. Lupei, A. Lupei, C. Tiseanu, S. Georgescu, C. Stoicescu, Phys. Rev. B 51 (1995) 8.
[10] M. Kuklja, J. Phys. Condens. Matter 12 (2000) 2953.
[11] C. Stanek, K. McClellan, M. Levy, R. Grimes, Phys. Status Solidi 243 (2006) R75.
[12] M. Nikl, A. Vedda, M. Fasoli, I. Fontana, V. Leguta., E. Mihokova, J. Pejchal, J. Rosa, K. Nejezchleb, Phys. Rev. B 76 (2007) 195121.
[13] W. Chewpradiktul, L. Świderski, M. Moszyński, IEEE Trans. Nucl. Sci. 56 (2009) 3800.
[14] C. Dujardin, C. Mancini, D. Amans, G. Ledoux, D. Abler, E. Auffray, P. Lecoq, D. Perrodin, A. Petrosyan, K. Ovanesyan, J. Appl. Phys. 108 (2010) 013510.
[15] M. Nikl, H. Ogino, A. Krasnikov, A. Beitlerova, Phys. Status Solidi A 202 (2005) 1113.
[16] H. Ogino, A. Yoshikawa, M. Nikl, A. Krasnikov, K. Kamada, J. Cryst. Growth 287 (2006) 309.
[17] J. Pejchal, M. Nikl, E. Mihokova, J. Mares, A. Yoshikawa, H. Ogino, K. Schillemat, A. Krasnikov, A. Vedda, K. Nejezchleb, V. Mucka, J. Phys. D: Appl. Phys. 42 (2009) 055117.
[18] W. Drozdowski, P. Dorenbos, J. de Hass, R. Drozdowska, A. Owens, K. Kamada, K. Tsutsumi, Y. Usuki, T. Yanagida, A. Yoshikawa, IEEE Trans. Nucl. Sci. 55 (2008) 2420.
[19] L. Swiderski, M. Moszynski, A. Nassalski, A. Syntfeld-Kazuch, T. Szczesniak, K. Kamada, K. Tsutsumi, Y. Usuki, T. Yanagida, A. Yoshikawa, IEEE Trans. Nucl. Sci. 56 (2009) 2499.
[20] W. Chewpraditkul, K. Sreebunpeng, M. Nikl, J. Mares, K. Nejezchleb, A. Phunpueok, C. Wanarak, Radiat. Meas. 47 (2012) 1.
[21] K. Kamada, T. Yanagida, T. Endo, K. Tsutumi, M. Yoshino, J. Kataoka, Y. Usuki, Y. Fujimoto, A. Fukabori, A. Yoshikawa, J. Cryst. Growth 352 (2012) 88.
[22] J. Mares, A. Beitlerova, M. Nikl, A. Vedda, C. D'Ambrosio, Phys. Status Solidi C 4 (2007) 996.
[23] I. Khodyuk, J. de Haas, P. Dorenbos, IEEE Trans. Nucl. Sci. 57 (2010) 1175.
[24] M. Derdzyan, K. Ovanesyan, A. Petrosyan, A. Belsky, C. Dujardin, C. Pedrini, E. Auffray, P. Lecoq, M. Lucchini., K. Pauwels, J. Cryst. Growth 361 (2012) 212.
[25] L. Boatner, J. Neal, J. Kolopus, J. Ramey, H. Akkurt, Nucl. Instrum. Methods Phys. Res. A 709 (2013) 138.
[26] K. Kamada, T. Yanagida, T. Endo, K. Tsutumi, Y. Fujimoto, A. Fukabori, A. Yoshikawa, J. Pejchal, M. Nikl, Cryst. Growth Des. 11 (2011) 4484.
[27] K. Kamada, T. Yanagida, J. Pejchal, M. Nikl, T. Endo, K. Tsutumi, Y. Fujimoto, A. Fukabori, A. Yoshikawa, J. Phys. D: Appl. Phys. 44 (2011) 505104.
[28] J. Udea, K. Aishima, S. Tanabe, Opt. Mater. 35 (2013) 1952.
[29] J. Ogieglo, A. Katelnikovas, A. Zych, T. Justel, A. Meijerink, J. Phys. Chem. A 117 (2013) 2479.
[30] M. Kucera., M. Nikl, M. Hanus, Z. Onderisinova, Phys. Status Solidi RRL 7 (2013) 571.
[31] U. Happek, J. Choi, A.M. Srivastava, J. Lumin. 94–95 (2001) 7.
[32] G. Blasse, B.C. Grabmaier, Luminescent Materials, Springer-Verlag, Berlin, 1994.
[33] M. Nikl, K. Kamada, S. Kurosawa, Y. Yokota, A. Yoshikawa, J. Pejchal, V. Babin, Phys. Status Solidi C 10 (2013) 172.
[34] V. Babin, M. Nikl, K. Kamada, A. Beitlerova, J. Phys. D: Appl. Phys. 46 (2013) 365303.
[35] Y. Wu, G. Ren, Opt. Mater. 35 (2013) 2146.
[36] A. de Vries, H. Kiliaan, G. Blasse, J. Solid State Chem. 65 (1986) 190.
[37] B. Di Bartolo, Energy Transfer Processes in Condensed Matter, Plenum Press, New York, 1984.
[38] D. Di Martino, A. Krasnikov, M. Nikl, K. Nitsch, A. Vedda, S. Zazubovich, Phys. Status Solidi A 201 (2004) R38.
[39] V. Babin, A. Krasnikov, J. Mares, M. Nikl, K. Nitsch, N. Solovieva, S. Zazubovich, Phys. Status Solidi A 196 (2003) 484.
[40] F. Kellendonk, G. Blasse, J. Chem. Phys. 75 (1981) 561.
[41] B. Di Bartolo, Spectroscopy of Solid-State Laser-Type Materials, Plenum Press, New York, 1987.
[42] M. Yokota, O. Taminoto, J. Phys. Soc. Jpn. 22 (1967) 779.
[43] M. Weber, Phys. Rev. B 4 (1971) 2932.
[44] V. Murk, N. Yaroshevich, J. Phys.: Condens. Matter 7 (1995) 5857.
[45] V. Babin, K. Blazek, A. Krasnikov, K. Nejezchleb, M. Nikl, Phys. Status Solidi C 2 (2005) 97.
[46] D.J. Robbins, J. Electrochem. Soc. 126 (1979) 1556.
[47] G. Blasse, Phys. Status Solidi A 73 (1982) 205.